Effect of 25-hydroxycholesterol in viral membrane fusion: Insights on HIV inhibition

Bárbara Gomes[a], Sónia Gonçalves[a], Anibal Disalvo[b], Axel Hollmann[a,b,c], Nuno C. Santos[a,*]

[a] Instituto de Medicina Molecular, Faculdade de Medicina, Universidade de Lisboa, Av. Prof. Egas Moniz, 1649-028 Lisbon, Portugal
[b] Laboratory of Biointerfaces and Biomimetic Systems, CITSE, University of Santiago del Estero, -CONICET, 4200 Santiago del Estero, Argentina
[c] Laboratory of Molecular Microbiology, Institute of Basic and Applied Microbiology, University of Quilmes, B1876BXD Bernal, Argentina

ARTICLE INFO

ABSTRACT

Recently, it was demonstrated that 25-hydroxycholesterol (25HC), an oxidized cholesterol derivative, inhibits human immunodeficiency virus type 1 (HIV) entry into its target cells. However, the mechanisms involved in this action have not yet been established. The aim of this work was to study the effects of 25HC in biomembrane model systems and at the level of HIV fusion peptide (HIV-FP). Integration of different biophysical approaches was made in the context of HIV fusion process, to clarify the changes at membrane level due to the presence of 25HC that result in the suppressing of viral infection.

Lipid vesicles mimicking mammalian and HIV membranes were used on spectroscopy assays and lipid monolayers in surface pressure studies. Peptide-induced lipid mixing assays were performed by Förster resonance energy transfer to calculate fusion efficiency. Liposome fusion is reduced by 50% in the presence of 25HC, comparatively to cholesterol. HIV-FP conformation was assessed by infrared assays and it relies on sterol nature. Anisotropy, surface pressure and dipole potential assays indicate that the conversion of cholesterol in 25HC leads to a loss of the cholesterol modulating effect on the membrane.

With different biophysical techniques, we show that 25HC affects the membrane fusion process through the modification of lipid membrane properties, and by direct alterations on HIV-FP structure. The present data support a broad antiviral activity for 25HC.

1. Introduction

Since the early 1980s, there have been several efforts to develop drugs against HIV [1,2]. The fusion between HIV and target cell membranes is a critical moment of the viral infection cycle. The binding of the viral envelope trimeric glycoprotein gp120 with host cell receptors (CD4 and CCR5 or CXCR4) represents the beginning of T CD4+ cells' infection. This interaction promotes a conformational transition in the viral glycoprotein gp41, which leads to an exposure of its hydrophobic N-terminal region, known as the HIV fusion peptide (HIV-FP). The two gp41 helical heptad repeat domains, the C terminal (CHR or HR2) and the N-terminal (NHR or HR1) fold into each other and form a hairpin-like structure. This approximates the cell and the viral membranes, promoting the formation of the fusion pore and the release of the viral content into the cell, where HIV-1 replication occurs [3]. Inhibition of this process could prevent all the subsequent intracellular steps.

Only two HIV entry inhibitors are available in the market: maraviroc, an inhibitor of gp120 binding to the CCR5 co-receptor [4], and enfuvirtide, a fusion inhibitor peptide that targets gp41 [5]. Despite this promising approach, little progress has been reported in developing longer action and orally bioavailable fusion inhibitors [2]. Furthermore, the drawbacks of these approaches include the emergence and selection of drug-resistant viruses [6]. Targeting less variable factors is an attractive concept that is less prone to drug-resistant viruses' selection. A particularly appealing notion is that viral membrane-targeting agents would necessarily limit the development of resistance, as it is not even conceivable how such resistance may develop. Thus, targeting

viral membranes represents an exciting new paradigm to explore regarding the development of broad-spectrum antivirals [7,8].

Several studies suggest that HIV fusion occurs in specialized plasma membrane microdomains, named lipid rafts. The definition of lipid raft is rather controversial, and there is no general agreement about it, mostly due to concept misinterpretations [9], or even about their existence *in vivo*. These domains are enriched in cholesterol and sphingomyelin, which emphasizes the importance of cholesterol on HIV entry [10–12]. However, the effects in this process of oxysterols such as 25-hydroxycholesterol (25HC, a cholesterol derivative presenting a second hydroxyl group at position 25) have not been totally clarified yet [13]. For several years, 25HC studies were focused on its influence in the development of atherosclerosis, since deregulation at the level of this sterol is associated with disease progression [14,15]. The hypothesis that 25HC could have a potential immune influence was hinted by the discovery that the enzyme responsible for its production, cholesterol-25-hydroxylase (CH25H), is expressed by macrophages and dendritic cells. In fact, CH25H is directly linked to interferons (IFN; agents from the innate immune system) activity, since it results from an IFN-stimulated gene. There are probably other enzymes with the capability to produce 25HC *in vitro*, but their role in generating this sterol *in vivo* is yet to be clarified [16].

In a study by Liu *et al.* [17], it was found that both the enzyme and 25HC present an extensive ability to neutralize the replication of enveloped viruses. 25HC blocked the entry of vesicular stomatitis virus and HIV in host cells. The authors suggested that 25HC suppresses viral growth by blocking the fusion between viral and cell membranes [17]. More recently, its capacity to block Zika virus infection at the same level was also demonstrated [18]. The hypothesis that the hydroxylation of cholesterol at carbon 25 turns it into a powerful antiviral mediator has gained interest in the last years [19,20]. However, to take advantage of this process, its mechanism of action needs to be understood.

The aim of this work was to address the effect of 25HC in the membranes fusion process. For this, we used synthetic HIV-FP, as well as small unilamellar vesicles (SUVs) and lipid monolayers as membrane model systems. Several biophysical studies were performed to understand the differences that occur at the membrane level when cholesterol is replaced by 25HC. The effect of binary lipid mixtures, with 25HC or cholesterol, on HIV-FP structure was evaluated. In our studies, we mimicked the conversion of cholesterol into 25HC, trying to define the changes at the membrane level that result in the possible mechanism of action of 25HC as viral fusion inhibitor.

2. Material and methods

2.1. Materials

POPC (1-palmitoyl-2-oleyl-*sn*-glycero-3-phosphocholine), DPPC (1,2-dipalmitoyl-*sn*-glycero-3-phosphocholine), POPE (1-palmitoyl-2-oleyl-*sn*-glycero-3-phosphoethanolamine), POPS (1-palmitoyl-2-oleyl-*sn*-glycero-3-phospho-L-serine), 25HC (25-hydroxycholesterol) and SM (egg sphingomyelin) were purchased from Avanti Polar Lipids (Alabaster, AL, USA). Cholesterol (Chol), DPH (1,6-diphenyl-1,3,5-hexatriene), TMA-DPH (4′-(trimethylammonio)diphenyl-hexatriene *p*-toluenesulfonate), laurdan (6-dodecanoyl-2-dimethylaminonaphthalene) and methyl-β-cyclodextrin (MBCD) were from Sigma-Aldrich (St. Louis, MO, USA). NBD-PE (1,2-dipalmitoyl-*sn*-glycero-3-phosphoethanolamine-*N*-(7-nitro-2-1,3-benzoxadiazol-4-yl)), Rhodamine-PE (Rhodamine B 1,2-dipalmitoyl-*sn*-glycero-3-phosphoethanolamine), di-8-ANEPPS and di-4-ANEPPDHQ were from Invitrogen (Eugene, OR, USA). The HIV fusion peptide (AVGIGALFLGFLGAAGSTMGAA), corresponding to the N-terminal domain of HIV-1 gp41 (HXB-2 viral clone) was synthesized by JPT (Berlin, Germany). Peptide stock solutions were prepared in dimethyl sulfoxide (DMSO). The working buffer used throughout the studies was HEPES 10 mM pH 7.4 in NaCl 150 mM.

2.2. Sample preparation

Small unilamellar vesicles were prepared by sonication, due to the impossibility to prepare oxysterols-containing vesicles by extrusion processes [21]. Briefly, a desired amount of lipids from chloroform stock solutions were mixed, and the solvent was evaporated under a nitrogen stream. HEPES buffer was added to resuspend the dispersion. SUVs were prepared by sonication in a water bath ultrasonicator for 10–15 min until the suspensions become transparent. Different compositions were prepared to mimic both mammalian cells and HIV membranes.

SUV stability and size distribution were evaluated by dynamic light scattering (DLS), using a Malvern Zetasizer NanoZS (Malvern, UK), guaranteeing a homogeneous vesicle size distribution regardless of lipid composition.

2.3. Lipid mixing assays

Membrane (hemi)fusion was measured by Förster resonance energy transfer (FRET), by incorporating two membrane probes in the SUV membrane: rhodamine B-PE and NBD-PE. This assay is based on the decrease in the efficiency of the resonance energy transfer between the two probes when the vesicles labelled mix with unlabelled vesicles. It is important to bear in mind that lipid mixing assays are not able to distinguish between membrane hemifusion and membrane fusion. This can only be fully established by using considerably more complex content mixing assays [22,23].

The concentration of each of the fluorescent probes within the pre-fusion liposome membrane was 0.6 mol%. Unlabelled SUVs were mixed with double-labelled SUVs in a 1:4 labelled:unlabelled proportion, at a total final lipid concentration of 100 μM, at 37 °C, under constant stirring. Fluorescence was measured with excitation at 470 nm and the emission scan between 500 and 650 nm. Excitation and emission slits were set to 10 nm. Lipid mixing, resulting from membrane fusion (or hemifusion), was quantified on a percentage basis according to equation [24,25]:

$$Fusion\ efficiency = \frac{R - R_0}{R_{100\%} - R_0} \tag{1}$$

where R is the ratio between the fluorescence intensity with emissions at 530 nm and 588 nm (corresponding to the fluorescence emission maxima of NBD and Rhodamine B, respectively) obtained 10 min after HIV-FP addition, R_0 is the ratio before peptide addition, and $R_{100\%}$ was set with vesicles labelled with 0.12 mol% of each of the fluorophores (one-fifth of the mol% of the previous measurements, corresponding therefore to a full lipid mixing between labelled and unlabelled vesicles).

2.4. FTIR-ATR spectroscopy

Infrared spectra were recorded on a Bruker Tensor 27 infrared spectrophotometer (Bruker Optik GmbH, Ettlingen, Germany) equipped with a Bio-ATR II accessory (ZnSe/silicon crystal). The spectrophotometer was continuously purged with dried air. Secondary structure of the HIV-FP was studied in the absence and presence of membranes with three lipid compositions: POPC, POPC:Chol (70:30) and POPC:25HC (70:30). SUVs 100 μM were incubated with HIV-FP 20 μM, in HEPES buffer, during 1 h, at 37 °C, under constant stirring.

A film with the samples was prepared by spreading the peptide/lipid solution on the plate under a stream of air to evaporate the solvent. Spectra were recorded at a spectral resolution of 4 cm^{-1} and 120 accumulations were performed per measurement. FTIR spectra were recorded at a wavelength range from 900 to 3500 cm^{-1}. Background of the internal reflection element was collected and subtracted to the samples. The obtained spectra were rescaled in the amide I area, between approximately 1600 and 1700 cm^{-1}.

2.5. Fluorescence anisotropy

DPH and TMA-DPH were dissolved in DMSO. SUVs of cell-like or HIV-like mixtures 3 mM were incubated for 30 min with each probe to achieve a final probe concentration of 0.33 mol%. DMSO concentration was kept below 2% (v/v). After the addition of the fluorescence probes, all samples were wrapped in aluminum foil and prepared in amber tubes to avoid bleaching. Steady-state fluorescence anisotropy, $\langle r \rangle$, was calculated as [26]:

$$\langle r \rangle = \frac{I_{vv} - I_{vh}}{I_{vv} - 2GI_{vh}} \tag{2}$$

where I_{vv} and I_{vh} are the parallel and perpendicular polarized fluorescence intensities measured with the vertically polarized excitation light and $G = I_{hv}/I_{hh}$ is an instrumental correction factor accounting for the polarization bias in the detection system. The excitation and emission wavelengths were, respectively, 350 nm and 432 nm for DPH and 355 nm and 430 nm for TMA-DPH. All measurements were performed at 37 °C in a Varian Cary Eclipse fluorescence spectrophotometer (Mulgrave, Australia).

2.6. Generalized polarization

Laurdan and di-4-ANEPPDHQ were dissolved in ethanol. SUVs of cell-like or HIV-like mixtures 3 mM were incubated for 30 min with each of the probe at 1:300 probe-to-lipid ratio. This ratio was chosen in order to increase the sensitivity of the measurements without perturbing the membrane properties [24,25]. The laurdan emission spectrum was measured from 370 to 600 nm, with excitation at 350 nm. The di-4-ANEPPDHQ emission spectrum was measured from 500 to 800 nm, with excitation at 488 nm. Generalized polarization, *GP*, was calculated as [27]:

$$GP = \frac{I_{ch1} - I_{ch2}}{I_{ch1} + I_{ch2}} \tag{3}$$

where I_{ch1} corresponds to the fluorescence intensity with emission at 435 nm for laurdan and 560 nm for di-4-ANEPPDHQ, and I_{ch2} corresponds to the intensity with emission at 500 nm for laurdan and 620 nm for di-4-ANEPPDHQ. All measurements were performed at 37 °C in a Varian Cary Eclipse fluorescence spectrophotometer.

2.7. Membrane cholesterol manipulation using MBCD

The time course of cholesterol exchange between SUVs and MBCD mixed with POPC, cholesterol or 25HC was carried out based on the shift of the emission spectra of the fluorescent dye laurdan. MBCD-lipid complexes (cholesterol acceptor) were prepared by premixing the lipid with MBCD as solids (weight ratio of 1:20) followed by solubilization in HEPES buffer. SUVs (cholesterol donor) of POPC and cholesterol (70:30) 1 mM were incubated for 30 min with laurdan at 1:300 probe-to-lipid ratio [28]. GP values were calculated at different time points before and after the addition of the MBCD-lipid complexes.

2.8. Surface pressure

Mixed or pure solutions of desirable lipid compositions were prepared from the respective stock solutions in chloroform and deposited onto a MilliQ water subphase with a Hamilton microsyringe, precise to 1.0 μL. After spreading, monolayers were left to equilibrate for 15 min before the compression was initiated, allowing the solvent to evaporate. In all experiments, monolayers were compressed with a barrier speed of 5 mm/min, which corresponds to a reduction of 0.1 Å^2/molecule/s. Π-A isotherms were recorded with a NIMA (UK) Langmuir trough (total area = 24,300 mm^2), equipped with two movable barrier, placed on an antivibration table. Surface pressure was measured with the accuracy of 0.1 mN/m, using a Wilhelmy plate made of platinum (KSV-NIMA)

connected to an electrobalance. The subphase temperature (20 °C) was controlled thermostatically to within 0.1 °C by a circulating water system. All experiments were repeated at least twice to ensure consistent results.

2.9. Membrane dipole potential assessment using di-8-ANEPPS

For lipid vesicles di-8-ANEPPS labelling, suspensions with 500 μM of total lipid were incubated overnight with 10 μM di-8-ANEPPS, to ensure maximum incorporation of the probe. Excitation spectra were obtained with 200 μM labelled-vesicles. Emission wavelength was set at 670 nm to avoid membrane fluidity-related artefacts. Excitation and emission slits for these measurements were set to 5 and 10 nm, respectively [29]. Differential excitation spectra were obtained by subtracting the excitation spectrum (normalized to the integrated areas) of labelled SUVs in the presence of sterols from the spectrum of POPC vesicles [30,31].

2.10. Data analysis

Fitting of the equations to the experimental data, was done by non-linear regression using Graphpad Prism 5. R^2 and residuals were evaluated in order to corroborate the accuracy of the fitting. Error bars on data presentation represent the standard error of mean (SEM) of at least three independent experiments.

3. Results and discussion

3.1. Membrane fusion efficiency

HIV-FP is a 23-residue peptide, corresponding to the fusion peptide domain from HIV gp41. Since there is a good correspondence between the vesicle fusion induced by HIV-FP and gp41-induced membrane fusion, studies with this peptide are a good approach to predict the fusion between the membranes of HIV and of its target cell [32–39]. POPC:-sterol SUVs were used on these experiments as a simplified model of mammalian cells. Whenever 25HC was increased, cholesterol concomitantly decreased by an equivalent percentage, in order to maintain a constant total sterol content and to simulate the *in vivo* conversion of cholesterol in 25HC by cholesterol-25-hydroxylase enzyme activity.

The lipid mixing assays showed a decrease of fusion efficiency of ~50% when all the cholesterol is substituted by 25HC, showing that the effects of 25HC occur at the membrane level (Fig. 1). In fact, at a HIV-FP/lipid concentration ratio of 0.2, the efficiency of the fusion between vesicles containing cholesterol reaches 80%, *versus* the 40% observed with just POPC and 25HC. Such results indicate that the complete conversion of cholesterol to 25HC, at the membrane level, can directly block the fusion promoted by HIV-FP.

3.2. HIV-FP structure

HIV gp41 fusion peptide activity depends on the lipid composition [40]. Thus, one might reason that the differences observed at the level of the membrane fusion experiments between cholesterol-containing and 25HC-containing membranes could be related to conformational changes on HIV-FP. Therefore, infrared spectroscopy was performed to determine the peptide structure in contact with membranes containing the two sterols, and to understand how the peptide structure could be correlated with its fusion activity. HIV-FP can adopt either α-helical or β-sheet conformation, and how membrane lipid composition affects the peptide secondary structure is still a matter of debate [40–44].

These measurements were performed in the absence and presence of lipid vesicles of POPC, POPC:Chol (70:30) and POPC:25HC (70:30). Since the major differences between the two binary systems in the lipid mixing assays were obtained with a HIV-FP/lipid concentration ratio of 0.2, the same proportion was applied (Fig. 2).
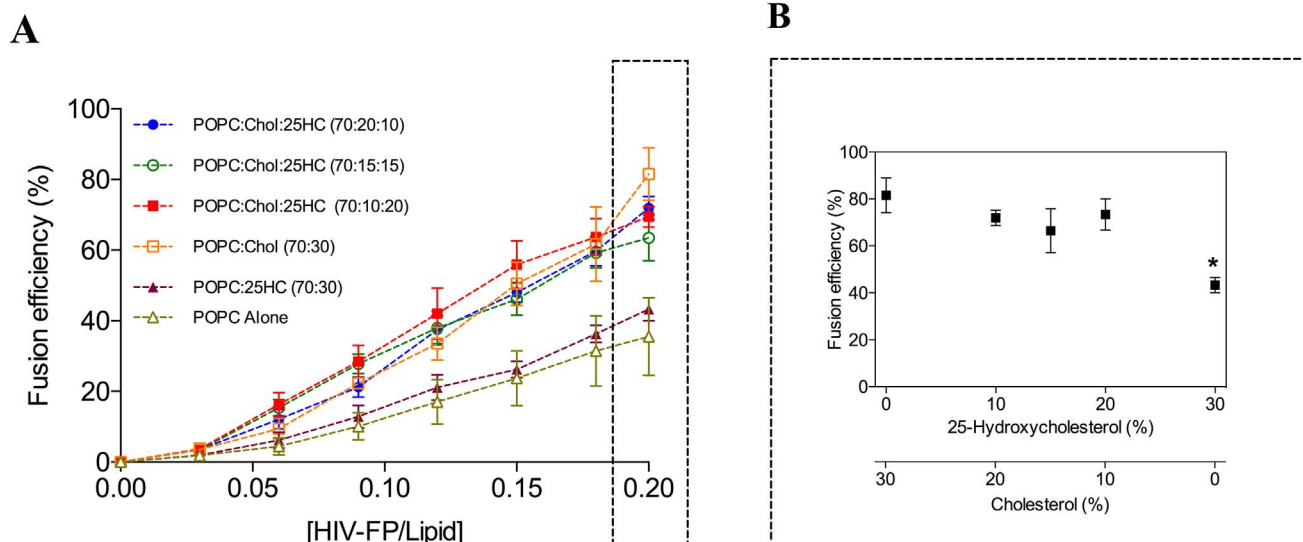
Fig. 1. Membrane fusion efficiency: (A) Fusion efficiency as a function of HIV-FP/lipid ratio for different membrane compositions: POPC:Chol:25HC (70:20:10) (filled circles), POPC:Chol:25HC (70:15:15) (open circles); POPC:Chol:25HC (70:10:20) (filled squares), POPC:Chol (70:30) (open squares), POPC:25HC (70:30) (filled triangles), POPC (open triangles). (B) Fusion efficiency at the higher HIV-FP/lipid ratio tested. Fusion efficiencies from binary samples present a statistically significant variation (*, $P < 0.05$, one-way ANOVA).
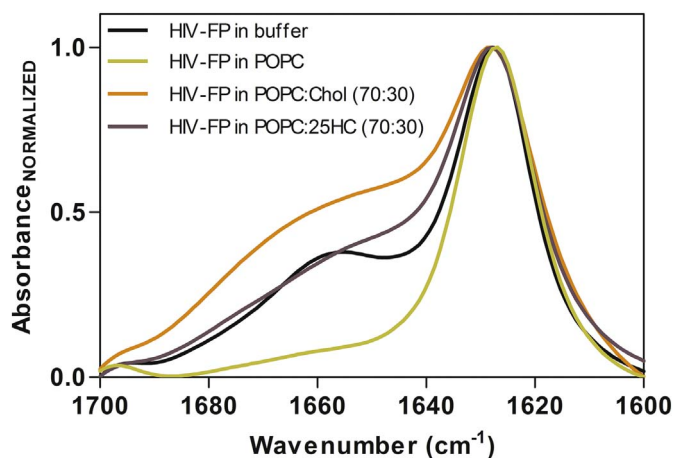

Fig. 2. FTIR-ATR spectra of HIV-FP in the presence of membranes with different lipid compositions. HIV-FP 20 μM was incubated with 100 μM SUVs during 1 h, at 37 °C, before spectra acquisition.

The peptide studied presents a different behavior depending on the lipid composition. With POPC, HIV-FP presents a prevalence of β-sheet conformation, characterized by a maximum at $1625 \, cm^{-1}$. When in contact with POPC:Chol vesicles, the peptide spectrum also presents contributions of the amide I band, at approximately $1660 \, cm^{-1}$, suggesting the presence of α-helical secondary structure [45]. Regarding 25HC, it is possible to observe an intermediate behavior. The β-sheet conformation is prevalent, as observed for the other compositions tested, and an α-helix contribution is also observed, but at lower extension than for the cholesterol-containing membranes.

Despite being a controversial subject for many years, several authors agree that the two secondary structures are necessary for an efficient fusion. According to Lai *et al.*, HIV-FP interacts and deeply inserts into the host cell membrane as a β-sheet, but then adopts an α-helical conformation to cross the lipid bilayer and promote the fusion pore formation [40,44]. Such hypothesis makes sense since it is more energetically favorable to cross the hydrophobic core of a lipid bilayer as an α-helix [46]. Conformational polymorphisms were also observed with fusion peptides from other enveloped viruses, such as influenza and paramyxoviruses, but in response to different environment triggers, namely pH and ionic strength changes [42,47]. This common ability of

viral fusion peptides to alter their secondary structure and depth of insertion indicates that structural plasticity is crucial for viral membrane fusion.

In the context of this work, we hypothesize that the conversion of cholesterol into 25HC renders the switching from β-sheet to α-helix less extensive, allowing the insertion of the fusion peptide into the membrane, but not the complete fusion. Further elucidation of the effects of 25HC on other viral fusion peptides structure is required to confirm the common mechanism for the broad-spectrum antiviral activity of this compound.

3.3. Effects on membrane rigidity and membrane packing

In order to identify the biophysical determinants of 25HC at the membrane level, fluorescence studies were performed. Fluorescence depolarization of the probes DPH and TMA-DPH was monitored to assess the effect of the conversion of cholesterol in 25HC on membrane fluidity [26]. Different cholesterol/25HC ratios were used on cell membrane-like (POPC/sterol) and HIV membrane-like (POPC/sterol/SM/DPPC/POPE/POPS) mixtures.

We observed an increase in anisotropy values in the presence of larger amounts of cholesterol, which increases the rigidity of membranes in the liquid state (such as POPC at room temperature), due to its compacting/ordering effect [48]. On the contrary, 25HC seems to maintain the intrinsic fluidity of the lipid membrane in the absence of cholesterol. In fact, the results obtained for vesicles with 25HC are very similar to those observed for pure POPC (Supplementary material), suggesting that this oxysterol does not have the membrane compacting ability typically found for cholesterol. However, the differences observed between the two sterols were more evident in the presence of DPH, which could be explained by the different in-depth membrane location of the two fluorescent probes: the hydrophobic core of the bilayer, where DPH is located, seems to be more sensitive to cholesterol compared to the polar membrane region closer to the lipid-water interface, sensed by TMA-DPH. Such results are similar to both models tested, mammalian cell-like and HIV-like membranes (Fig. 3).

With the purpose of complementing the anisotropy data, we also determined the order parameter *GP*. Two fluorescent probes were used for this purpose: laurdan and di-4-ANEPPDHQ. Both probes operate by the same mechanism, sensing the reorientation of solvent dipoles, which is related to water penetration and lipid packing, though their
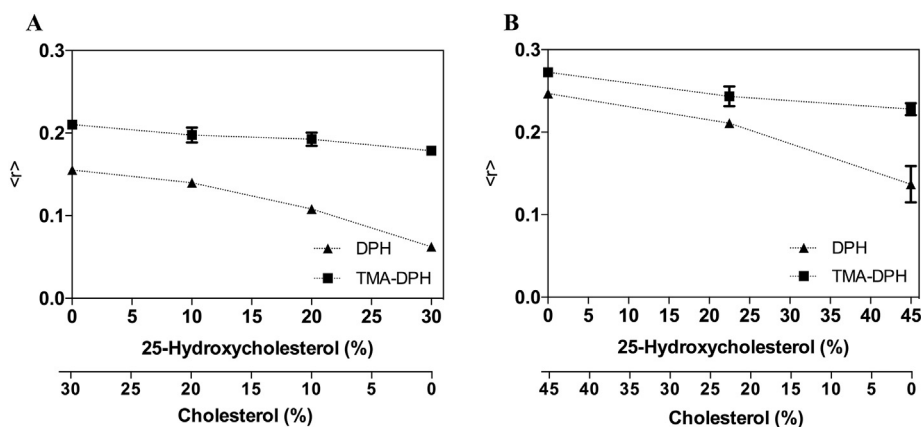
Fig. 3. DPH (filled triangles) and TMA-DPH (filled squares) fluorescence anisotropy as a function of 25HC/cholesterol content. (A) Anisotropy changes in cell membrane-like SUVs. (B) Anisotropy changes in HIV membrane-like SUVs.
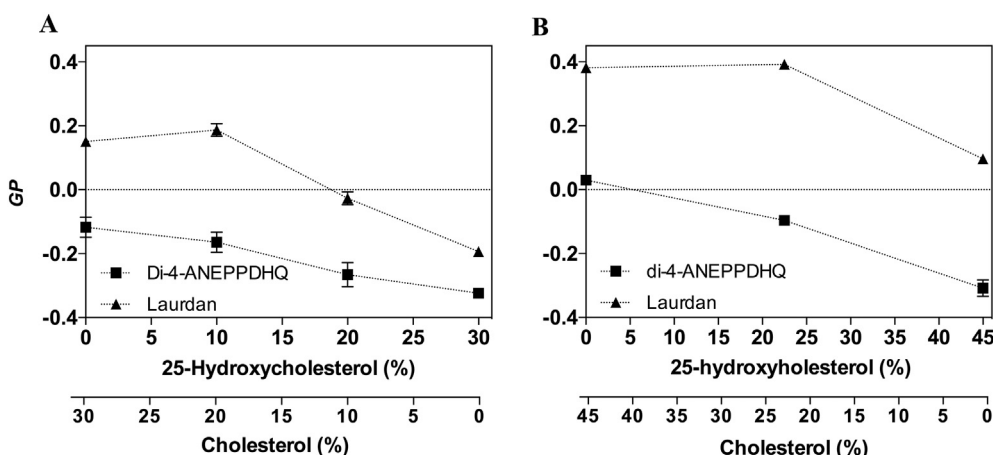

Fig. 4. Membrane-ordering effects measured by generalized polarization for laurdan (filled triangles) and di-4-ANEPPDHQ (filled squares) on cell membrane-like (A) and HIV membranelike (B) SUVs.

location is different [49,50]. The fluctuation on *GP* values reports the variances on the local packing of the membrane [51]. In this case, a progressive enrichment in 25HC, substituting cholesterol, led to a decrease on *GP* values, indicating that the membranes with 25HC are less packed than those with the same amount of cholesterol (Fig. 4).

The *GP* values obtained for pure POPC SUVs (Supplementary material) are comparable to those determined for POPC:25HC (70:30), indicating a similar membrane packing.

3.4. Membrane cholesterol manipulation using MBCD

The use of methyl-β-cyclodextrin is the preferential method to manipulate the level of cholesterol in membranes, due to the high rate of cholesterol exchange between the two systems [52]. For SUVs of POPC:Chol (70:30), *GP* changes can be directly used to assess cholesterol content [53,54]. Incubation of MBCD–25HC and MBCD–POPC with the referred SUVs resulted in cholesterol transfer to the MBCD complex, as shown by the decrease on *GP*, which demonstrates the decrease on lipid packing. On the contrary, the addition of the MBCD-cholesterol complex to POPC:Chol (70:30) liposomes promotes the enrichment of cholesterol content in the membrane, leading to higher *GP* values (Fig. 5).

The equilibrium of cholesterol exchange between MBCD and SUVs was established instantly, as demonstrated by the constant *GP* values SUVs at extended incubation times [52]. These experiments show that the conversion between both sterols deeply change the membrane order and are a good predictor of dynamic changes within biological membranes.
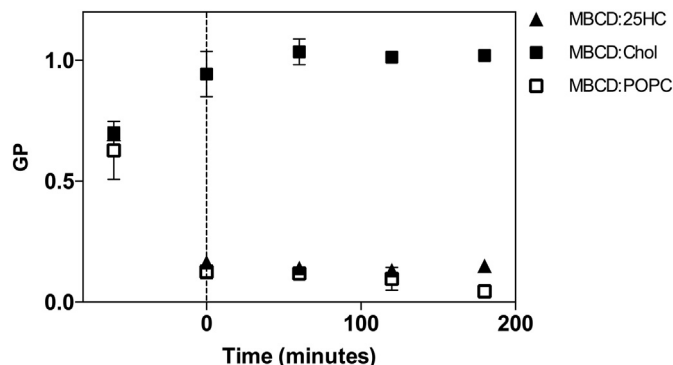

Fig. 5. Changes in laurdan *GP* value for SUVs of POPC and cholesterol incubated with different MBCD-lipid complexes: MBCD:25HC (filled triangles), MBCD:Chol (filled squares) and MBCD:POPC (open squares). The dotted line indicates the addition of MBCD-lipid complex.

3.5. Surface pressure

In order to complement the previous information, pressure–area isotherms for pure POPC, binary mixtures of POPC:25HC (70:30), POPC:Chol (70:30) and ternary mixture of POPC:Chol:25HC (70:15:15) were obtained (Fig. 6).

From these isotherms, we could further confirm that membranes made with 25HC instead of cholesterol present a different behavior. A detailed examination of the isotherm at low pressures (Fig. 6C)
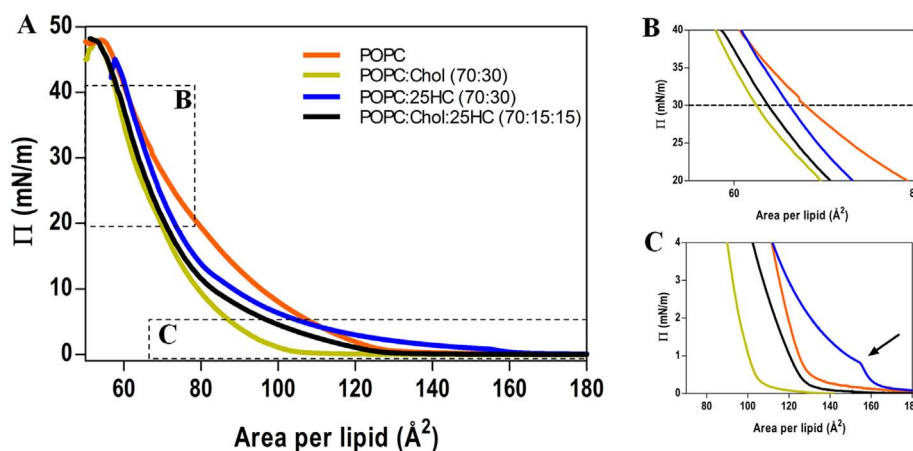
Fig. 6. Surface pressure–area isotherm for POPC and POPC:sterol monolayers (A). Insets highlight the pressure–area isotherms at high (B) and low (C) pressures, otherwise unclear in the main figure. The arrow in the pressure–area isotherm at low pressures highlights the kink present on POPC:25HC monolayer curve.

highlights the presence of a kink (arrow) for the POPC:25HC mixture, as previously reported for DMPC and DPPC binary mixtures [55,56], corresponding to the onset of the two phase region of the mixture. However, in the context of our work, a detailed analysis at higher pressures, comparable with those found in lipids bilayers, close to 30 mN/m (Fig. 6B) [57,58], we found that the monolayers with 25HC exhibit a behavior much more comparable with pure POPC than with the binary mixture with cholesterol. In terms of area per lipid, it seems that at high pressures the condensation effect on POPC, typically found for cholesterol, is less noticeable for 25HC. Interestingly, when a ternary mixture was evaluated, the behavior of the monolayers, especially at high pressures, seems to be more similar to POPC:Chol. The ternary mixtures present an area per lipid lower than the POPC:25HC monolayers, indicating the occurrence of a condensing effect as observed for binary mixtures of POPC:Chol.

The relation between rigidity and membrane fusion was studied by several authors, which concluded that cholesterol is essential for membrane fusion between HIV and the target cell [59–63]. According to Apellániz et al. [63], rigidification of POPC vesicles, with sequential additions of cholesterol, sharply increases the efficiency of membrane fusion. As membranes in which cholesterol was replaced by 25HC exhibit higher fluidity, due to a lack of the compacting effect promoted by cholesterol, the changes in this property may explain the results obtained in our lipid mixing assays, as well as in the biological assays demonstrating that the presence of 25HC or of the enzyme that leads to its production (CH25H) have an extensive ability to neutralize the replication of enveloped viruses [17]. Such results can be even more important in the context of lipid rafts, lipid domains rich in cholesterol, presenting a crucial role in some viral infections [10–12].

3.6. Membrane dipole potential changes

The fluorescence sensor di-8-ANEPPS was used to monitor the variations on the membrane dipole potential. Lipid vesicles with five different compositions were evaluated, with different amounts of cholesterol and/or 25-hydroxycholesterol.

When the total membrane dipole moment changes, a shift in the excitation spectrum maximum occurs, which is usually measured as a differential excitation spectra. The differential excitation spectra shown in Fig. 7A reveal opposite behaviors for cholesterol and 25HC. In agreement with previous reports [64], the differential excitation spectra showed that cholesterol increases the magnitude of the membrane dipole potential of POPC vesicles, with a maximum around 450 nm. Interestingly, the effect of 25HC is the opposite, with a red-shifted maximum.

Fluorescence intensity ratios can be calculated using two different

excitation wavelengths, corresponding to the minimum and the maximum of the differential spectra. Fig. 7B represents the values of the fluorescence intensity ratio, R, as a function of 25HC concentration in vesicles. The higher R is observed for cholesterol-rich vesicles, in contrast with 25HC-rich membranes [31,65,66].

It is important to correlate these results with those from the lipid mixing assays. Buzon et al. showed that the interaction of HIV-FP with model membranes is affected by the membrane dipole potential [67]. According to the authors, membranes with higher membrane dipole potential induce an increase in lipid mixing rates, due to an increased affinity of the HIV-FP to the membranes. The same trend was also observed in our study: the HIV-FP presents lower affinity for membranes where cholesterol was replaced by 25HC, probably due to their lower membrane dipole potential. The decreased peptide-membrane affinity may reduce the lipid mixing rates and, consequently, the fusion between vesicles.

4. Conclusion

The mechanism underlying the inhibition of enveloped viruses by 25HC is still far from being understood. In the present work, we used different biophysical techniques to study how the conversion of cholesterol in 25HC affects the membrane properties, impairing membrane fusion, a crucial step for the viral life cycle.

First, we demonstrated that the presence of 25HC, instead of cholesterol, can block the membrane fusion catalyzed by HIV-FP and, therefore, HIV entry into a target cell. The changes observed on the HIV-FP secondary structure indicate that the presence of 25HC could decrease the ability of the peptide to promote the formation of the fusion pore, by losing part of its conformational plasticity, a required feature among different viral fusion peptides [40,42,47]. Moreover, the lower affinity between the peptide and 25HC-rich membranes, explained by differences on dipole potential, also contributes to the low fusion efficiency.

In parallel, the alteration of some of the intrinsic biophysical properties of biological membranes, such as fluidity and ordering, indicates that the conversion of cholesterol in 25HC leads to a loss of the typical cholesterol membrane modulating effect. Such property is crucial for viral replication, and its impairment results in the blocking of virus-cell fusion.

In conclusion, our data indicate that the addition of a single hydroxyl group on cholesterol deeply changes the biophysical properties of the membrane, resulting in a lower affinity and structural plasticity of the HIV fusion peptide, both critical factors in the fusion process. Furthermore, our results demonstrate that this antiviral agent targets the membrane lipids themselves, and not another viral or target cell
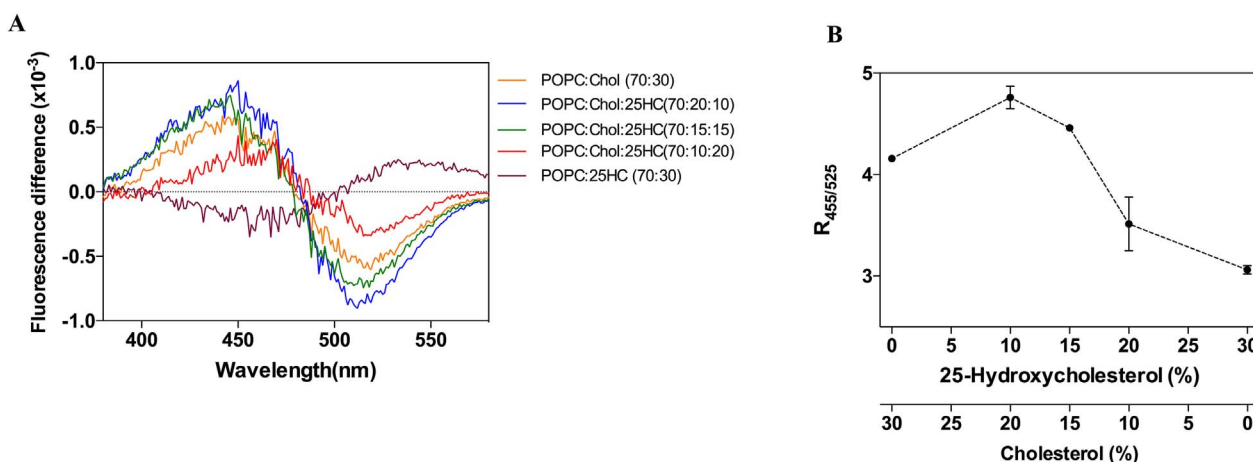
Fig. 7. Membrane dipole changes detected by di-8-ANEPPS fluorescence (A) differential excitation spectra of di-8-ANEPPS bound to membranes in the presence of different percentages of 25HC and/or cholesterol. (B) Influence of 25HC/cholesterol content on the membrane dipole potential, assessed with the fluorescent probe di-8-ANEPPS, presented as the fluorescence ratio R455/525.

component absent from the simple system tested. The findings from our studies suggest that 25HC can also modulate the behavior of viral membranes, which could affect not only viral entry but also viral integrity and function, since cholesterol-depleted viral particles show reduced infectivity [12]. However, how to apply the knowledge obtained regarding 25HC to turn this compound into a therapeutic agent is a major question. The diversity of cholesterol functions in cells, from membranes integrity to cell signaling, impairs the use of 25HC as single oxysterol [68]. The developed strategy should turn 25HC more specific towards the target, which may be accomplished by combining 25HC with other molecules, namely other types of membrane fusion inhibitors [69]. Overall, these conclusions indicate that several enveloped viruses, and not just HIV, may be affected by 25HC through the same mechanism, making this compound a broad-spectrum viral fusion inhibitor, as suggested by previous *in vitro* and *in vivo* studies [17,18,70].

Supplementary data to this article can be found online at https://doi.org/10.1016/j.bbamem.2018.02.001.

Conflict of interest

The authors declare that they have no conflicts of interest with the contents of this article.

Transparency document

The Transparency document associated with this article can be found, in online version.

References

[1] E. De Clercq, Anti-HIV drugs: 25 compounds approved within 25 years after the discovery of HIV, Int. J. Antimicrob. Agents 33 (2009) 307–320.

[2] D.R. Kuritzkes, HIV-1 entry inhibitors: an overview, Curr. Opin. HIV AIDS 4 (2009) 82–87.

[3] R. Blumenthal, S. Durell, M. Viard, HIV entry and envelope glycoprotein-mediated fusion, J. Biol. Chem. 287 (2012) 40841–40849.

[4] S.S. Lieberman-Blum, H.B. Fung, J.C. Bandres, Maraviroc: a CCR5-receptor antagonist for the treatment of HIV-1 infection, Clin. Ther. 30 (2008) 1228–1250.

[5] T. Matthews, M. Salgo, M. Greenberg, J. Chung, R. DeMasi, D. Bolognesi, Enfuvirtide: the first therapy to inhibit the entry of HIV-1 into host CD4

[6] lymphocytes, Nat. Rev. Drug Discov. 3 (2004) 215–225.

[6] G.B. Melikyan, Driving a wedge between viral lipids blocks infection, Proc. Natl. Acad. Sci. U. S. A. 107 (2010) 17069–17070.

[7] F. Vigant, M. Jung, B. Lee, Positive reinforcement for viruses, Chem. Biol. 17 (2010) 1049–1051.

[8] F. Vigant, N.C. Santos, B. Lee, Broad-spectrum antivirals against viral fusion, Nat. Rev. Microbiol. 13 (2015) 426–437.

[9] J. Bernardino de la Serna, G.J. Schutz, C. Eggeling, M. Cebecauer, There is no simple model of the plasma membrane organization, Front. Cell Dev. Biol. 4 (2016) 106.

[10] S.T. Yang, V. Kiessling, J.A. Simmons, J.M. White, L.K. Tamm, HIV gp41-mediated membrane fusion occurs at edges of cholesterol-rich lipid domains, Nat. Chem. Biol. 11 (2015) 424–431.

[11] T. Takahashi, T. Suzuki, Function of membrane rafts in viral lifecycles and host cellular response, Biochem. Res. Int. 2011 (2011) 245090.

[12] S.M. Campbell, S.M. Crowe, J. Mak, Lipid rafts and HIV-1: from viral entry to assembly of progeny virions, J. Clin. Virol. 22 (2001) 217–227.

[13] M.S. Freitas, C. Follmer, L.T. Costa, C. Vilani, M.L. Bianconi, C.A. Achete, J.L. Silva, Measuring the strength of interaction between the Ebola fusion peptide and lipid rafts: implications for membrane fusion and virus infection, PLoS One 6 (2011).

[14] A.J. Brown, W. Jessup, Oxysterols and atherosclerosis, Atherosclerosis 142 (1999) 1–28.

[15] F. Wang, W. Xia, F. Liu, J. Li, G. Wang, J. Gu, Interferon regulator factor 1/retinoic inducible gene I (IRF1/RIG-I) axis mediates 25-hydroxycholesterol-induced interleukin-8 production in atherosclerosis, Cardiovasc. Res. 93 (2012) 190–199.

[16] U. Diczfalusy, On the formation and possible biological role of 25-hydroxycholesterol, Biochimie 95 (2013) 455–460.

[17] S.Y. Liu, R. Aliyari, K. Chikere, G.M. Li, M.D. Marsden, J.K. Smith, O. Pernet, H.T. Guo, R. Nusbaum, J.A. Zack, A.N. Freiberg, L.S. Su, B. Lee, G.H. Cheng, Interferon-inducible cholesterol-25-hydroxylase broadly inhibits viral entry by production of 25-hydroxycholesterol, Immunity 38 (2013) 92–105.

[18] C. Li, Y.Q. Deng, S. Wang, F. Ma, R. Aliyari, X.Y. Huang, N.N. Zhang, M. Watanabe, H.L. Dong, P. Liu, X.F. Li, Q. Ye, M. Tian, S. Hong, J. Fan, H. Zhao, L. Li, N. Vishlaghi, J.E. Buth, C. Au, Y. Liu, N. Lu, P. Du, F.X. Qin, B. Zhang, D. Gong, X. Dai, R. Sun, B.G. Novitch, Z. Xu, C.F. Qin, G. Cheng, 25-Hydroxycholesterol protects host against Zika virus infection and its associated microcephaly in a mouse model, Immunity 46 (2017) 446–456.

[19] D. Lembo, V. Cagno, A. Civra, G. Poli, Oxysterols: an emerging class of broad spectrum antiviral effectors, Mol. Asp. Med. 49 (2016) 23–30.

[20] J.G. Cyster, E.V. Dang, A. Reboldi, T. Yi, 25-Hydroxycholesterols in innate and adaptive immunity, Nat. Rev. Immunol. 14 (2014) 731–743.

[21] J.C. Verhagen, P. ter Braake, J. Teunissen, G. van Ginkel, A. Sevanian, Physical effects of biologically formed cholesterol oxidation products on lipid membranes investigated with fluorescence depolarization spectroscopy and electron spin resonance, J. Lipid Res. 37 (1996) 1488–1502.

[22] P.M. Matos, M. Marin, B. Ahn, W. Lam, N.C. Santos, G.B. Melikyan, Anionic lipids are required for vesicular stomatitis virus G protein-mediated single particle fusion with supported lipid bilayers, J. Biol. Chem. 288 (2013) 12416–12425.

[23] S. Padilla-Parra, P.M. Matos, N. Kondo, M. Marin, N.C. Santos, G.B. Melikyan, Quantitative imaging of endosome acidification and single retrovirus fusion with distinct pools of early endosomes, Proc. Natl. Acad. Sci. U. S. A. 109 (2012) 17627–17632.

[24] A. Hollmann, M.A. Castanho, B. Lee, N.C. Santos, Singlet oxygen effects on lipid membranes: implications for the mechanism of action of broad-spectrum viral fusion inhibitors, Biochem. J. 459 (2014) 161–170.

[25] M. Muller, O. Zschornig, S. Ohki, K. Arnold, Fusion, leakage and surface hydrophobicity of vesicles containing phosphoinositides: influence of steric and electrostatic effects, J. Membr. Biol. 192 (2003) 33–43.

[26] B.R. Lentz, Membrane fluidity as detected by diphenylhexatriene probes, Chem.

Phys. Lipids 50 (1989) 171–190.

[27] H.J. Kaiser, D. Lingwood, I. Leventhal, J.L. Sampaio, L. Kalvodova, L. Rajendran, K. Simons, Order of lipid phases in model and plasma membranes, Proc. Natl. Acad. Sci. U. S. A. 106 (2009) 16645–16650.

[28] S.L. Niu, D.C. Mitchell, B.J. Litman, Manipulation of cholesterol levels in rod disk membranes by methyl-beta-cyclodextrin: effects on receptor activation, J. Biol. Chem. 277 (2002) 20139–20145.

[29] M.T. Augusto, A. Hollmann, M.A.R.B. Castanho, M. Porotto, A. Pessi, N.C. Santos, Improvement of HIV fusion inhibitor C34 efficacy by membrane anchoring and enhanced exposure, J. Antimicrob. Chemother. 69 (2014) 1286–1297.

[30] P.M. Matos, H.G. Franquelim, M.A. Castanho, N.C. Santos, Quantitative assessment of peptide-lipid interactions. Ubiquitous fluorescence methodologies, Biochim. Biophys. Acta 1798 (2010) 1999–2012.

[31] E. Gross, R.S. Bedlack Jr., L.M. Loew, Dual-wavelength ratiometric fluorescence measurement of the membrane dipole potential, Biophys. J. 67 (1994) 208–216.

[32] D.P. Weliky, Solid-state NMR structural measurements and models of the HIV and influenza fusion proteins in membranes, Biophys. J. 106 (2014) 636a–637a.

[33] F.B. Pereira, F.M. Goni, A. Muga, J.L. Nieva, Permeabilization and fusion of un-charged lipid vesicles induced by the HIV-1 fusion peptide adopting an extended conformation: dose and sequence effects, Biophys. J. 73 (1997) 1977–1986.

[34] S.R. Durell, I. Martin, J.M. Ruysschaert, Y. Shai, R. Blumenthal, What studies of fusion peptides tell us about viral envelope glycoprotein-mediated membrane fu-sion (review), Mol. Membr. Biol. 14 (1997) 97–112.

[35] M. Pritsker, J. Rucker, T.L. Hoffman, R.W. Doms, Y. Shai, Effect of nonpolar sub-stitutions of the conserved Phe11 in the fusion peptide of HIV-1 gp41 on its func-tion, structure, and organization in membranes, Biochemistry 38 (1999) 11359–11371.

[36] E.O. Freed, E.L. Delwart, G.L. Buchschacher Jr., A.T. Panganiban, A mutation in the human immunodeficiency virus type 1 transmembrane glycoprotein gp41 dom-inantly interferes with fusion and infectivity, Proc. Natl. Acad. Sci. U. S. A. 89 (1992) 70–74.

[37] M.D. Delahunty, I. Rhee, E.O. Freed, J.S. Bonifacino, Mutational analysis of the fusion peptide of the human immunodeficiency virus type 1: identification of cri-tical glycine residues, Virology 218 (1996) 94–102.

[38] W. Qiang, D.P. Weliky, HIV fusion peptide and its cross-linked oligomers: efficient syntheses, significance of the trimer in fusion activity, correlation of beta strand conformation with membrane cholesterol, and proximity to lipid headgroups, Biochemistry 48 (2009) 289–301.

[39] E.M. Reuven, Y. Dadon, M. Viard, N. Manukovsky, R. Blumenthal, Y. Shai, HIV-1 gp41 transmembrane domain interacts with the fusion peptide: implication in lipid mixing and inhibition of virus-cell fusion, Biochemistry 51 (2012) 2867–2878.

[40] A.L. Lai, A.E. Moorthy, Y. Li, L.K. Tamm, Fusion activity of HIV gp41 fusion domain is related to its secondary structure and depth of membrane insertion in a choles-terol-dependent fashion, J. Mol. Biol. 418 (2012) 3–15.

[41] W. Qiang, Y. Sun, D.P. Weliky, A strong correlation between fusogenicity and membrane insertion depth of the HIV fusion peptide, Proc. Natl. Acad. Sci. U. S. A. 106 (2009) 15314–15319.

[42] H. Yao, M. Hong, Membrane-dependent conformation, dynamics, and lipid inter-actions of the fusion peptide of the paramyxovirus PIV5 from solid-state NMR, J. Mol. Biol. 425 (2013) 563–576.

[43] W.T. Heller, D.K. Rai, Changes in lipid bilayer structure caused by the helix-to-sheet transition of an HIV-1 gp41 fusion peptide derivative, Chem. Phys. Lipids 203 (2017) 46–53.

[44] A.L. Lai, J.H. Freed, HIV gp41 fusion peptide increases membrane ordering in a cholesterol-dependent fashion, Biophys. J. 106 (2014) 172–181.

[45] A. Barth, Infrared spectroscopy of proteins, Biochim. Biophys. Acta 1767 (2007) 1073–1101.

[46] S. Jayasinghe, K. Hristova, S.H. White, Energetics, stability, and prediction of transmembrane helices, J. Mol. Biol. 312 (2001) 927–934.

[47] Y. Sun, D.P. Weliky, 13C-13C correlation spectroscopy of membrane-associated influenza virus fusion peptide strongly supports a helix-turn-helix motif and two turn conformations, J. Am. Chem. Soc. 131 (2009) 13228–13229.

[48] T. Rog, M. Pasenkiewicz-Gierula, I. Vattulainen, M. Karttunen, Ordering effects of cholesterol and its analogues, Biochim. Biophys. Acta 1788 (2009) 97–121.

[49] T. Parasassi, M. Di Stefano, M. Loiero, G. Ravagnan, E. Gratton, Influence of

[50] cholesterol on phospholipid bilayers phase domains as detected by Laurdan fluor-escence, Biophys. J. 66 (1994) 120–132.

J. Dinic, H. Biverstahl, L. Maler, I. Parmryd, Laurdan and di-4-ANEPPDHQ do not respond to membrane-inserted peptides and are good probes for lipid packing, Biochim. Biophys. Acta 1808 (2011) 298–306.

[51] S.A. Sanchez, M.A. Tricerri, E. Gratton, Laurdan generalized polarization fluctua-tions measures membrane packing micro-heterogeneity in vivo, Proc. Natl. Acad. Sci. U. S. A. 109 (2012) 7314–7319.

[52] S.L. Niu, B.J. Litman, Determination of membrane cholesterol partition coefficient using a lipid vesicle-cyclodextrin binary system: effect of phospholipid acyl chain unsaturation and headgroup composition, Biophys. J. 83 (2002) 3408–3415.

[53] S.A. Sanchez, G. Gunther, M.A. Tricerri, E. Gratton, Methyl-beta-cyclodextrins preferentially remove cholesterol from the liquid disordered phase in giant uni-lamellar vesicles, J. Membr. Biol. 241 (2011) 1–10.

[54] S.A. Sanchez, M.A. Tricerri, E. Gratton, Interaction of high density lipoprotein particles with membranes containing cholesterol, J. Lipid Res. 48 (2007) 1689–1700.

[55] B.L. Stottrup, L.H. Hernandez-Balderrama, J.C. Kunz, A.H. Nguyen, B.J. Sonquist, Comparison of cholesterol and 25-hydroxycholesterol in phase-separated langmuir monolayers at the air-water interface, J. Phys. Chem. B 118 (2014) 11231–11237.

[56] B.L. Stottrup, S.L. Keller, Phase behavior of lipid monolayers containing DPPC and cholesterol analogs, Biophys. J. 90 (2006) 3176–3183.

[57] J. Seelig, P.M. Macdonald, P.G. Scherer, Lipid polar groups as indicators of electric charge and regulators of membrane-surface potential, Biol. Chem. Hoppe Seyler 368 (1987) 1272.

[58] J.M. Smaby, M. Momsen, V.S. Kulkarni, R.E. Brown, Cholesterol-induced interfacial area condensations of galactosylceramides and sphingomyelins with identical acyl chains, Biochemistry 35 (1996) 5696–5704.

[59] K.E. Zawada, D. Wrona, R.J. Rawle, P.M. Kasson, Influenza viral membrane fusion is sensitive to sterol concentration but surprisingly robust to sterol chemical iden-tity, Sci. Rep. 6 (2016) 29842.

[60] S.T. Yang, A.J. Kreutzberger, J. Lee, V. Kiessling, L.K. Tamm, The role of cholesterol in membrane fusion, Chem. Phys. Lipids 199 (2016) 136–143.

[61] R.C. Aloia, H. Tian, F.C. Jensen, Lipid composition and fluidity of the human im-munodeficiency virus envelope and host cell plasma membranes, Proc. Natl. Acad. Sci. U. S. A. 90 (1993) 5181–5185.

[62] M. Viard, I. Parolini, M. Sargiacomo, K. Fecchi, C. Ramoni, S. Ablan, F.W. Ruscetti, J.M. Wang, R. Blumenthal, Role of cholesterol in human immunodeficiency virus type 1 envelope protein-mediated fusion with host cells, J. Virol. 76 (2002) 11584–11595.

[63] B. Apellaniz, E. Rujas, P. Carravilla, J. Requejo-Isidro, N. Huarte, C. Domene, J.L. Nieva, Cholesterol-dependent membrane fusion induced by the gp41 mem-brane-proximal external region-transmembrane domain connection suggests a me-chanism for broad HIV-1 neutralization, J. Virol. 88 (2014) 13367–13377.

[64] T. Asawakarn, J. Cladera, P. O'Shea, Effects of the membrane dipole potential on the interaction of saquinavir with phospholipid membranes and plasma membrane receptors of Caco-2 cells, J. Biol. Chem. 276 (2001) 38457–38463.

[65] J.C. Franklin, D.S. Cafiso, Internal electrostatic potentials in bilayers: measuring and controlling dipole potentials in lipid vesicles, Biophys. J. 65 (1993) 289–299.

[66] R.J. Clarke, Effect of lipid structure on the dipole potential of phosphatidylcholine bilayers, Biochim. Biophys. Acta 1327 (1997) 269–278.

[67] V. Buzon, J. Cladera, Effect of cholesterol on the interaction of the HIV GP41 fusion peptide with model membranes. Importance of the membrane dipole potential, Biochemistry 45 (2006) 15768–15775.

[68] P. Goluszko, B. Nowicki, Membrane cholesterol: a crucial molecule affecting in-teractions of microbial pathogens with mammalian cells, Infect. Immun. 73 (2005) 7791–7796.

[69] B. Gomes, N.C. Santos, M. Porotto, Biophysical properties and antiviral activities of measles fusion protein derived peptide conjugated with 25-hydroxycholesterol, Molecules 22 (2017).

[70] Y. Chen, S. Wang, Z. Yi, H. Tian, R. Aliyari, Y. Li, G. Chen, P. Liu, J. Zhong, X. Chen, P. Du, L. Su, F.X. Qin, H. Deng, G. Cheng, Interferon-inducible cholesterol-25-hy-droxylase inhibits hepatitis C virus replication via distinct mechanisms, Sci. Rep. 4 (2014) 7242.